Amazon River enhances diazotrophy and carbon sequestration in the tropical North Atlantic Ocean

A. Subramaniam*†, P. L. Yager‡, E. J. Carpenter§, C. Mahaffey¶, K. Björkman‖, S. Cooley‡, A. B. Kustka**, J. P. Montoya††, S. A. Sañudo-Wilhelmy‡‡, R. Shipe§§, and D. G. Capone‡‡

*Lamont–Doherty Earth Observatory, Columbia University, Palisades, NY 10964; ‡Department of Marine Sciences, University of Georgia, Athens, GA 30602; §Romberg Tiburon Center, San Francisco State University, Tiburon, CA 94920; ¶Department of Earth and Ocean Science, University of Liverpool, Liverpool L69 3GP, United Kingdom; ‖Department of Oceanography, SOEST, University of Hawaii, Honolulu, HI 96822; **Institute of Marine and Coastal Sciences, Rutgers, The State University of New Jersey, New Brunswick, NJ 08901; ††School of Biology, Georgia Institute of Technology, Atlanta, GA 30332; ‡‡Wrigley Institute for Environmental Studies and Department of Biological Sciences, University of Southern California, Los Angeles, CA 90089; and §§Department of Ecology and Evolutionary Biology and Institute of the Environment, University of California, Los Angeles, CA 90095

Edited by David M. Karl, University of Hawaii, Honolulu, HI, and approved April 24, 2008 (received for review October 29, 2007)

The fresh water discharged by large rivers such as the Amazon is transported hundreds to thousands of kilometers away from the coast by surface plumes. The nutrients delivered by these river plumes contribute to enhanced primary production in the ocean, and the sinking flux of this new production results in carbon sequestration. Here, we report that the Amazon River plume supports N_2 fixation far from the mouth and provides important pathways for sequestration of atmospheric CO_2 in the western tropical North Atlantic (WTNA). We calculate that the sinking of carbon fixed by diazotrophs in the plume sequesters 1.7 Tmol of C annually, in addition to the sequestration of 0.6 Tmol of C yr^{-1} of the new production supported by NO_3 delivered by the river. These processes revise our current understanding that the tropical North Atlantic is a source of 2.5 Tmol of C to the atmosphere [Mikaloff-Fletcher SE, *et al.* (2007) Inverse estimates of the oceanic sources and sinks of natural CO_2 and the implied oceanic carbon transport. *Global Biogeochem Cycles* 21, doi:10.1029/2006GB002751]. The enhancement of N_2 fixation and consequent C sequestration by tropical rivers appears to be a global phenomenon that is likely to be influenced by anthropogenic activity and climate change.

diatom diazotroph associations | nitrogen fixation | new production | river plumes | *Richelia*

Downward vertical transport of organic carbon produced by phytoplankton, referred to as the biological pump, is a mechanism that transfers carbon from the surface to the deep ocean and regulates atmospheric CO_2 (1). The flux of nitrate (NO_3) from deep water to the photic zone can stimulate new phytoplankton production and export (2), but because the upwelling or diffusive flux of NO_3 is accompanied by a corresponding upward flux of CO_2, its net contribution to removal of carbon from the atmosphere is much reduced. However, the sinking flux due to new production associated with nitrogenous inputs from rivers, atmospheric deposition, and N_2 fixation (diazotrophy), results in the net transport of atmospheric carbon to the deep ocean (3), or "carbon sequestration" (4).

The Amazon River has the largest discharge of any river and accounts for 18% of all of the riverine input to the oceans. Between May and September, the Amazon plume covers up to 1.3×10^6 km^2 with a freshwater lens of salinity <35 [supporting information (SI) Table S1], which accounts for 20% of the WTNA. Our understanding of the influence of the Amazon River on the carbon cycle in the WTNA has evolved significantly since Ryther *et al.* (5) first suggested that the Amazon River depressed the productivity of the region influenced by its plume. Several studies have focused on the nutrients delivered by the river to the inner shelf, the subsequent river-supported new production of 0.6 Tmol of C yr^{-1} [based on the $NO_3 + NO_2 + NH_4$ flux of 2.5×10^8 mol of N d^{-1} reported by DeMaster and Aller (6)] and consequences to biogeochemical cycles [reviewed by DeMaster and Aller (6)]. However, none of these investigations studied the plume in the open ocean beyond the shelf. We undertook three field campaigns to study the influence of the Amazon River on the carbon and nitrogen cycles beyond the shelf. Samples at a total of 82 stations in the WTNA in January to February 2001, July to August 2001, and April to May 2003 (Fig. 1 and Table S2) complement earlier studies by examining the region of the plume starting 300 km north of the mouth of the river. We classified the stations into three categories based on sea surface salinity (SSS).[¶¶] The "low salinity" group contained all of the stations with SSS <30. Stations that had SSS between 30 and 35 were classified as "mesohaline," whereas those with SSS >35 were classified as "oceanic."

Surface NO_3 concentrations were below detection at most stations, with the highest value of 0.50 μM recorded at the station with the lowest salinity of 24. DeMaster and Pope (7) found when plotting NO_3 vs. soluble reactive phosphorus (SRP) concentrations for samples taken from outside the river mouth and adjacent shelf, the SRP concentration was 0.14 μM at the zero NO_3 intercept, implying that the Amazon is an important source of "excess" SRP (N:P < 16) to the WTNA. Using SRP concentration in the river, Devol (8) calculated that the Amazon contributed ≈30% of global riverine SRP flux to the ocean. This is very likely an underestimate because it does not include the contribution of SRP desorbed from particles once the river water mixes with oceanic waters (9). Although we do not know enough about P-uptake dynamics of the endosymbiotic diazotrophic cyanobacteria *Richelia*, *Trichodesmium* is capable of using dissolved organic P in the form of monophosphate esters and phophonates (10) in addition to the SRP supplied by the river. The Amazon is also very likely an important source of labile Fe to WTNA. Boyle *et al.* (11) found that >90% of the dissolved Fe (dFe) in river water flocculated and precipitated in estuaries upon mixing with seawater. However, even if only 1% of the 2.5 μM dFe reported by Bergquist and Boyle (12) at Macapá was transported offshore by the plume, the surface concentrations in the offshore plume could be 25 times higher than concentrations typically observed in the WTNA. The concentrations of SRP (<52 nM) and dFe (<1.8 nM) we measured in the outer plume

Author contributions: A.S., P.L.Y., E.J.C., S.A.S.-W., and D.G.C. designed research; A.S., P.L.Y., E.J.C., C.M., K.B., S.C., A.B.K., R.S., and D.G.C. performed research; A.S. and S.A.S.-W. contributed new reagents/analytic tools; A.S., P.L.Y., C.M., K.B., S.C., J.P.M., S.A.S.-W., R.S., and D.G.C. analyzed data; and A.S., P.L.Y., E.J.C., C.M., and D.G.C. wrote the paper.

The authors declare no conflict of interest.

This article is a PNAS Direct Submission.

Freely available online through the PNAS open access option.

†To whom correspondence should be addressed at: LDEO/Columbia University, 61 Route 9W, Palisades, NY 10964. E-mail: ajit@ldeo.columbia.edu.

¶¶Salinity was measured by using the Practical Salinity Scale and has no units.

This article contains supporting information online at www.pnas.org/cgi/content/full/0710279105/DCSupplemental.

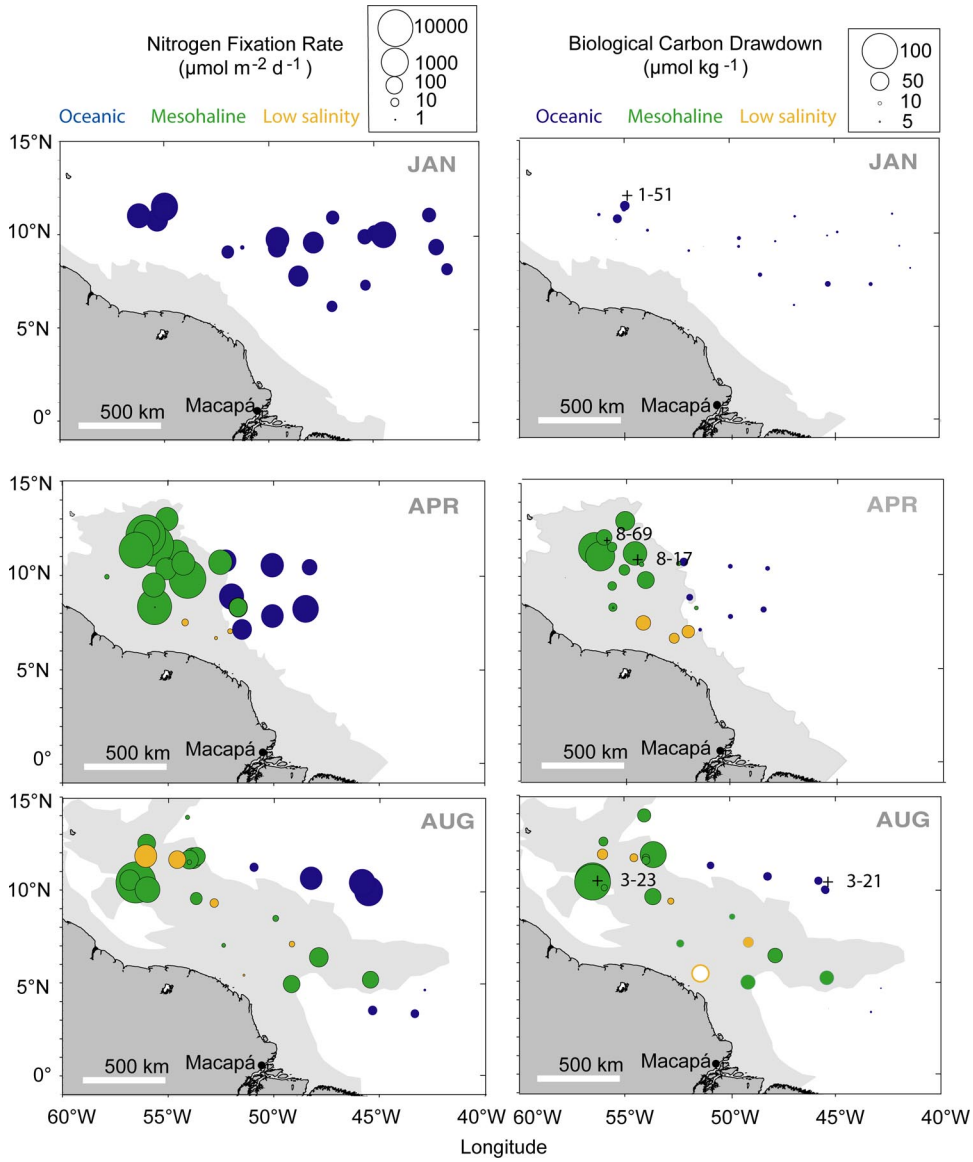

Fig. 1. Maps showing locations for N_2 fixation and DIC drawdown measurements. (*Left*) Total N_2-fixation rates for *Trichodesmium* and *Richelia* (μmol of N m^{-2} d^{-1}) by cruise. The Amazon plume (salinity <35) is shaded in gray. The areas of the circles are proportional to the rates. (*Right*) Surface dissolved inorganic carbon drawdown (μmol of C kg^{-1}); the location of the shallow traps are indicated with station number. The white-filled circle indicates negative values or carbon excess.

(Table 1; and see Fig. 3) were much lower than the 0.8 and 2.5 μM, respectively, reported near the mouth, reflecting mixing with ocean waters, uptake by phytoplankton, and complex particle adsorption/desorption relationships that need to be investigated in the future. Aerosols are also important sources of Fe to this region (13), and there is little evidence of Fe limitation in the WTNA, with average surface concentrations exceeding the half-saturation constant for growth of coastal diatoms as well as for N_2 fixation by *Trichodesmium* (0.05–0.075 nM and 0.16 nM, respectively (14, 15). After the plume leaves the continental shelf, excess P and Si (N:P $<$ 16 and Si:n $>$ 6.6) supplied by the river establish an ideal niche for N_2 fixation.

The mean depth-integrated primary production rate for the coastal stations was 35 $\pm$ 5 mmol of C $m^{-2}d^{-1}$, the lowest rate of the three station groups (Table 1). We found that colored dissolved organic matter, rather than phytoplankton, dominated ($\approx$70%) total light absorption at coastal stations, whereas phytoplankton and other particulate matter dominated ($\approx$40% each) absorption in the mesohaline stations (16), extending the conclusion of Smith *et al.* (17) that primary production on the Amazon shelf is light-limited nearshore (Fig. 2). The depth-integrated primary production rates for the mesohaline and oceanic stations were comparable with each other at $\approx$58 mmol of C $m^{-2}d^{-1}$. The mean depth-integrated N_2 fixation rate (μmol of N $m^{-2}d^{-1}$) of mesohaline stations (986 $\pm$ 373, n = 34), however, was more than six times higher than that of the oceanic stations (157 $\pm$ 32, n = 39, Fig. 1) with the highest rates measured at stations dominated by *Richelia* blooms. Assuming Redfield stoichiometry in the organic matter produced, these observed rates of N_2 fixation can support only 11% of the observed total primary production (6.5 of 57 mmol of C $m^{-2}d^{-1}$) in the mesohaline waters, whereas $\approx$2% and <0.5% of the primary production was supported by N_2 fixation in oceanic stations and low-salinity stations, respectively. Pico- and nanoplanktonic N_2 fixers were not found to be abundant in mesohaline waters (18), and their contribution to this system is not yet well constrained.

The phytoplankton species composition at the low-salinity stations was dominated by coastal diatom species such as *Skel-*

Table 1. Forcing factors and biological response at the three station types

Parameter	Low-salinity stations	Mesohaline stations	Oceanic stations	Kruskal–Wallis *P*
Surface salinity	27.91 ± 0.63 (0,3,5) = 8	32.97 ± 0.20 (0,18,17) = 35	36.03 ± 0.03 (24,7,8) = 39	4.9×10^{-15}
1% light depth, m	28 ± 4 (0,3,5) = 8	37 ± 3 (0,18,17) = 35	86 ± 3 (24,7,8) = 39	6.1×10^{-12}
Surface dissolved iron, nM	1.8 ± 0.4 (0,3,4) = 7	1.7 ± 0.2 (0,17,8) = 25	1.4 ± 0.5 (17,7,2) = 26	0.006
Surface soluble reactive phosphorus, nM	52 ± 18 (0,3,5) = 8	30 ± 4 (0,16,15) = 31	37 ± 4 (19,7,5) = 31	0.35
Surface dissolved Si, μM	10.9 ± 2.7 (0,3,5) = 8	4.1 ± 0.7 (0,15,12) = 27	1.4 ± 0.1 (16,6,3) = 25	9.8×10^{-5}
Surface biogenic silica, μmol liter^{-1}	0.47 ± 0.19 (0,2,5) = 7	0.53 ± 0.12 (0,17,12) = 29	0.08 ± 0.03 (12,6,3) = 21	4.5×10^{-6}
Depth integrated *Trichodesmium* counts ($\times 10^6$ trichomes m^{-2})	12 ± 9 (0,3,5) = 8	13 ± 4 (0,18,16) = 34	28 ± 5 (24,7,8) = 39	0.027
Depth integrated *Richelia* counts ($\times 10^6$ heterocysts m^{-2})	7 ± 6 (0,3,5) = 8	523 ± 116 (0,18,16) = 34	4 ± 2 (24,7,8) = 39	9.2×10^{-6}
Depth-integrated chlorophyll *a*, mg of chla m^{-2}	14 ± 2 (0,3,5) = 8	22 ± 2 (0,17,17) = 34	26 ± 1 (21,6,8) = 35	0.002
Depth-integrated primary production, mmol of C m^{-2} day	35 ± 5 (0,3,5) = 8	57 ± 7 (0,17,12) = 29	59 ± 3 (19,7,5) = 31	0.010
Depth-integrated N_2 fixation by *Trichodesmium* and *Richelia*, μmol of N m^{-2} day	25 ± 17 (0,3,5) = 8	986 ± 373 (0,18,16) = 34	157 ± 32 (24,7,8) = 39	0.028
Surface biologically depleted DIC, μmol kg^{-1}	20 ± 10 (0,3,5) = 8	29 ± 5 (0,16,16) = 32	12 ± 1 (22,7,8) = 37	1.8×10^{-6}
Shallow trap mass flux, mg m^{-2} day	—	152 ± 26 (0,3,5) = 8	42 ± 8 (2,0,3) = 5	—

Mean measurements ± SE (number of stations from the January, April, and July cruises, respectively) = Total. The data for each station are provided in Table S2. The Kruskal–Wallis *P* value is shown for the null hypothesis that all samples are drawn from the same population.

etonema costatum and *Pseudonitzschia* sp (19). The diatoms *Hemiaulus hauckii* and *Rhizosolenia clevei* containing the symbiotic cyanobacteria *Richelia* sp. (diatom diazotroph associations, DDA) formed ≈28% of the biomass at the mesohaline stations, whereas they comprised <2% of biomass at the oceanic and low-salinity stations. We posit that the composition of the

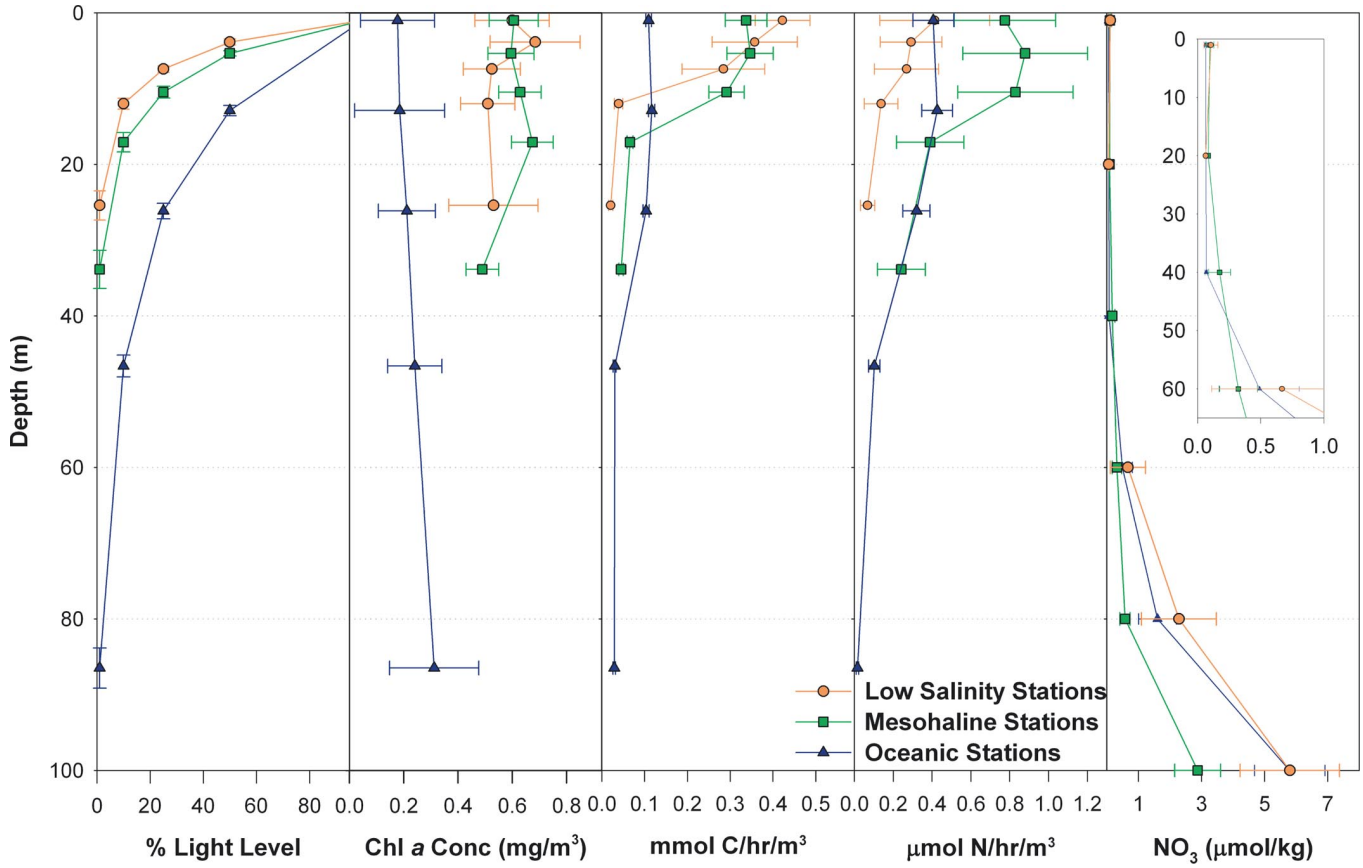

Fig. 2. Vertical profiles of mean light depths, chlorophyll a concentration, C and N fixation rates, and NO_3 concentrations binned by station type, details shown in Table S2. The error bars represent standard error.

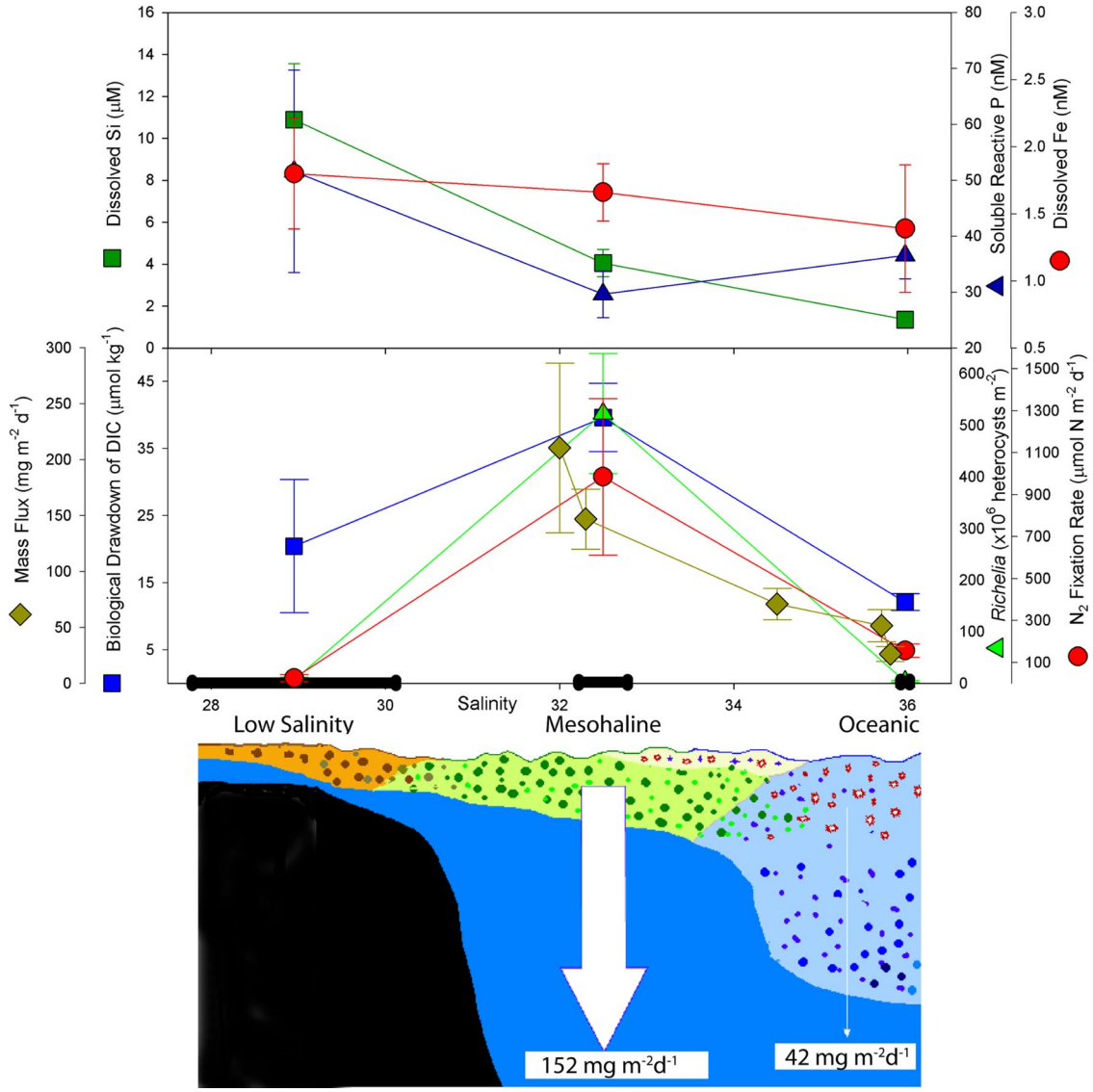

Fig. 3. Changes along the river plume as it moves offshore. (*Top*) Changes in surface nutrient concentrations as a function of salinity for each of the station types; the values and statistics are presented in Table 1. Error bars denote standard error; the thick horizontal line on the *x* axis indicates the mean salinity ±1 S.E. for each group of stations. (*Middle*) Changes in biological response and mass flux from floating sediment traps at 200 m presented as in *A*. (*Bottom*) A schematic of changes along the plume; the arrows showing the mean mass flux for the mesohaline, and oceanic stations. The brown particles represent coastal phytoplankton species; the dark green represents DDA; the red represents *Trichodesmium*; and the blue represents particles typical of oligotrophic oceanic phytoplankton. Phytoplankton chlorophyll, *Trichodesmium*, and *Richelia* concentrations are given in Table 1. Water below the euphotic zone is depicted in solid dark blue, and the 1% light depths are given in Table 1.

phytoplankton community changes along the Amazon River plume from the mouth to the open ocean in response to changing nutrient availability (Fig. 3). At the low-salinity stations, there is enough P, Si, and combined N at the surface to support coastal diatom species, and there is very little N_2 fixation. As the combined N is assimilated and the plume is mixed with low-nutrient ocean waters, diazotrophs become significant sources of new nitrogen (Table 1 and Fig. 1). Diatom hosts of *Richelia*, the dominant diazotroph at the mesohaline stations, require the Si and P found in the river plume, but N is supplied by fixation of dinitrogen (N_2). Farther "downstream," where river-associated Si and SRP are depleted, the species composition transitions to that typical of oligotrophic tropical oceans, and the dominant diazotroph is *Trichodesmium*.

The change in phytoplankton community structure affects the efficiency of the biological pump. Although new nitrogen provided by any marine diazotroph increases the availability of fixed nitrogen in the ocean and leads to carbon sequestration, the actual pathways and time scales of sinking of organic matter through the upper ocean and into the deep sea can vary for the different diazotrophs (20). We found a significant correlation between biologically depleted DIC in the plume (Fig. 1) and the vertically integrated cell abundance of *Richelia* ($r = 0.6$; $n = 77$, $P < 0.01$). The six surface samples with the greatest net seasonal biological pCO_2 drawdown (100–130 μatm) were associated with large blooms of *Richelia.* Other plume stations with no prevailing diazotroph population or with *Trichodesmium* showed much smaller (20–40 μatm) seasonal biological drawdowns (21). These conclusions were further supported by a multivariate statistical approach: A principal-components analysis (Table S3) generated four axes that explained 74% of the system variability. Axis 1 (35%) signified the physical river–ocean gradient, Axis 2

(19%) denoted the mesohaline DDA population, Axis 3 (13%) represented *Trichodesmium* population, and Axis 4 (7%) correlated with total integrated primary production and dFe. The key result was that the largest nonconservative changes in DIC were associated with high *Richelia* abundance and high N_2 fixation on Axis 2 (Fig. S1).

The DDA drawdown of DIC corresponded to greater particulate export. Sedimentation rates (mg m^{-2} d^{-1}) derived by using floating sediment traps at 200 m were nearly fourfold higher at our mesohaline stations (152 ± 26, eight samples from three deployments) compared with oceanic stations (42 ± 8, 5 samples from two deployments, Wilcoxon rank sum $P = 0.003$, Fig. 3). The isotopic composition of N in the material collected in the floating trap can be used to infer the potential origin of the material found in the traps. Particulate nitrogen in waters dominated by both *Trichodesmium* and the diatom *Hemiaulus* containing the endosymbiont *Richelia* is known to be significantly depleted in ^{15}N (22), with $\delta^{15}N$ values typically being <0‰. At our mesohaline station (3–23, shown in Fig. 1) dominated by DDAs, the $\delta^{15}N$ of the trap material was −1.5‰, suggesting that the DDA contributed strongly to the vertical flux. The high particulate export by DDAs has also been observed deeper in the water column. In the subtropical Pacific, Scharek *et al.* (23) reported a 500- to 1,250-fold increase of intact DDA cells at 4,000 m in late July/early August. They calculated that these DDAs had settling rates of 100–200 m d^{-1} with little remineralization along the way. Deuser *et al.* (24) observed that total material flux into a deep trap (3200 m) deployed just east of Barbados (13°13′ N, 57°41′ W) ranged between 100 and 200 mg $m^{-2}d^{-1}$ when the Amazon River plume passed over it but was only 35–60 mg $m^{-2}d^{-1}$ during the winter months, analogous to our mesohaline and oceanic conditions, respectively.

One important consequence of the rapid sinking of diatoms is the significant transport of atmospheric C to the deep ocean by this process. Using a 6.6 C/N stoichiometry and the mean N_2 fixation rate for mesohaline stations dominated by DDAs, we derive a C-fixation rate of 6.5 (±2.5) mmol of C m^{-2} d^{-1} for diazotrophs in the waters influenced by the Amazon plume. Combining this with satellite-based monthly estimates of the areal extent of the plume with salinity between 30 and 35, we calculate that the carbon sequestration due to diazotrophy in mesohaline waters can be as high as 1.7 ± 0.7 Tmol of C (20 ± 8 Tg of C) annually. Added to the estimate for new production based on river nitrate, we get a total Amazon-supported new production of 2.3 Tmol of C per yr^{-1}. Despite differences in relevant temporal and spatial scales, the mesohaline number agrees well with the independent net community production estimate of 1.2 ± 0.4 (25) or 1.3 ± 0.5 (26) Tmol of C (15 ± 6 Tg of C), calculated from the drawdown of DIC in the plume and 1.3 Tmol of C (15 Tg of C) derived by using a mass flux of 150 mg $m^{-2}d^{-1}$ and by assuming that 40% of total sinking material is organic carbon (Table S1) and suggests that this biological pump is highly efficient.

Our work shows that the Amazon River plays an important role in enhancing primary production far beyond the continental shelf by supporting diazotrophs and thereby providing a significant source of new N. Although the Amazon represents the largest riverine input to the tropical ocean, there are numerous other tropical rivers that deliver large volumes of water with "excess" P and Si to this biome. Carbon sequestration by DDAs associated with excess nutrients supplied by tropical river plumes may be a globally significant phenomenon. *Hemiaulus* with N_2-fixing symbionts have been reported in Mediterranean sapropels related to hypermonsoonal periods of enhanced runoff of the Nile River (27). In the Eastern Tropical Atlantic, up to 95% of the cells at a station south of the Congo River mouth were *Hemiaulus* (28). Studies in the South China Sea (29) have reported enhanced N_2 fixation in mesohaline waters. Tropical mesohaline waters are an important interface between terrestrial and oceanic realms. The occurrence and impact of N_2 fixation in these waters is sensitive to changes in hydrological cycles, fertilizer, and land use and must be understood.

Methods Summary

The abundances and depth distribution of the diazotroph population at each station was determined as described by Carpenter *et al.* (30). The euphotic depth was estimated from spectral downwelling irradiance measured by using a free-falling spectroradiometer. Measurements of C and N fixation, chlorophyll *a* concentrations, and phytoplankton biomass were integrated through the euphotic zone to determine the areally integrated rates reported in Table 1 and in Table S2. Carbon fixation was determined by ^{14}C uptake method (30) and N_2 fixation by both ^{15}N uptake and C_2H_2 reduction methods (31). Chlorophyll a concentrations were measured by using an HPLC (32). Fe concentrations were determined by AAS (MP01, MP03) or ICP-MS (MP08) after preconcentration with APDC/DDDC organic extraction (34). SRP was quantified spectrophotometrically (35). Si and NO_3 were determined by using standard calorimetric techniques on a Bran and Luebbe AA3. Total dissolved inorganic carbon and alkalinity were measured by using standard methods (33), and biological drawdown calculated as described by (26). Please see SI *Text* for detailed description of methods.

ACKNOWLEDGMENTS. K.B. and C.M. thank D. Karl for support in preparation of this manuscript. We thank J. Burns, S. Govil, T. Gunderson, and M. Neumann for their assistance in sample collection and analysis, the anonymous referees for their suggestions, Dr. S. Holland for consulting on statistics, and A. Stach for helping with Fig. 3. Shiptime and much of the fieldwork was funded by two U.S. National Science Foundation (NSF) Biocomplexity in the Environment grants. A.S., D.G.C., and E.J.C. had additional support from the National Aeronautics and Space Administration (NASA) Ocean Biology Program and a SIMBIOS grant; P.L.Y. was supported by a U.S. Department of Energy Office of Science grant, a National Oceanic and Atmospheric Administration Office of Global Programs grant, and by faculty research support from the University of Georgia; J.P.M. was supported by the NSF Ocean Sciences Program; S.R.C. was additionally supported by fellowships from the University of Georgia and NASA Earth System Science; and R.S. was supported by a fellowship from the Wrigley Institute and C.M. by a fellowship from the University of Southern California Women in Science and Engineering Program for portions of this research. This is LDEO contribution 7179.

1. Gruber N, Sarmiento JL (2002) in *The Sea*, eds Robinson AR, McCarthy JJ, Rothschild BJ (Wiley, New York), pp 337–399.
2. Dugdale RC, Goering JJ (1967) Uptake of new and regenerated forms of nitrogen in primary productivity. *Limnol Oceanogr* 12:196–206.
3. Eppley RW, Peterson BJ (1979) Particulate organic matter flux and planktonic new production in the deep ocean. *Nature* 282:677–680.
4. Dilling L, *et al.* (2003) The role of carbon cycle observations and knowledge in carbon management. *Annu Rev Environ Res* 28:521–558.
5. Ryther JH, Menzel DW, Corwin N (1967) Influence of the Amazon River outflow on the ecology of the western tropical Atlantic. I. Hydrography and nutrient chemistry. *J Mar Res* 25:69–83.
6. DeMaster DJ, Aller RC (2001) in *Biogeochemistry of Major World Rivers*, eds Degens ET, Kempe S, Richey JE (Wiley, New York), pp 323–347.
7. Demaster DJ, Pope RH (1996) Nutrient dynamics in Amazon Shelf waters—Results from Amasseds. *Continent Shelf Res* 16:263–289.
8. Devol AH, Richey JE, Forsberg BR (1991) in *Phosphorus Cycles in Terrestrial and Aquatic Ecosystems, Regional Workshop 3: South and Central America*, eds Tiessen H, Lopez-Hernandez D, Salcedo IH (SCOPE/UNEP Proceedings, University of Saskatchewan, Saskatoon, Canada), pp 9–23.
9. Chase EM, Sayles FL (1980) Phosphorus in suspended sediments of the Amazon River. *Estuar Coast Mar Sci* 11:383–391.
10. Dyhrman ST, *et al.* (2006) Phosphonate utilization by the globally important marine diazotroph *Trichodesmium*. *Nature* 439:68–71.
11. Boyle EA, Edmond JM, Sholkovitz ER (1977) The mechanism of iron removal in estuaries. *Geochim Cosmochim Acta* 41:1313–1324.
12. Bergquist BA, Boyle EA (2006) Iron isotopes in the Amazon River system: Weathering and transport signatures. *Earth Planet Sci Lett* 248:54–68.
13. Chen Y, Siefert RL (2004) Seasonal and spatial distributions and dry deposition fluxes of atmospheric total and labile iron over the tropical and subtropical North Atlantic Ocean. *J Geophys Res Atmos* 109:doi:10.1029/2003JD003958.

14. Sunda WG, Huntsman SA (1995) Iron uptake and growth limitation in oceanic and coastal phytoplankton. *Mar Chem* 50:189–206.
15. Berman-Frank I, Cullen J, Hareli Y, Sherrell R, Falkowski PG (2001) Iron availability, cellular iron quotas, and nitrogen fixation in *Trichodesmium*. *Limnol Oceanogr* 46:1249–1277.
16. Del Vecchio R, Subramaniam A (2004) Influence of the Amazon River on the surface optical properties of the Western Tropical North Atlantic Ocean. *J Geophys Res* 109:doi:10.1029/2004JC002503.
17. Smith WO, Jr, DeMaster DJ (1996) Phytoplankton biomass and productivity in the Amazon River plume: Correlation with seasonal river discharge. *Continent Shelf Res* 6:227–244.
18. Foster RA, *et al.* (2007) Influence of the Amazon River plume on distributions of free-living and symbiotic cyanobacteria in the western tropical North Atlantic Ocean. *Limnol Oceanogr* 52:517–532.
19. Shipe RF, Curtaz J, Subramaniam A, Carpenter EJ, Capone DG (2006) Diatom biomass and productivity in oceanic and plume influenced waters of the western tropical Atlantic Ocean. *Deep Sea Res Part I* 53:1320–1334.
20. Montoya J, Carpenter E, Capone D (2002) Nitrogen fixation and nitrogen isotope abundance in zooplankton of the oligotrophic North Atlantic. *Limnol Oceanogr* 47:1617–1628.
21. Cooley SR, Yager PL (2006) Physical and biological contributions to the Western Tropical North Atlantic Ocean carbon sink formed by the Amazon River Plume. *J Geophys Res, C* 111 doi:10.1029/2005JC002954.
22. Carpenter EJ, *et al.* (1999) Extensive bloom of a N2-fixing diatom/cyanobacterial association in the tropical Atlantic Ocean. *Mar Ecol Progress Ser* 185:273–283.
23. Scharek R, Tupas LM, Karl DM (1999) Diatom fluxes to the deep sea in the oligotrophic North Pacific gyre at Station ALOHA. *Mar Ecol Progress Ser* 182:55–67.
24. Deuser WG, Muller-Karger FE, Hemleben C (1988) Temporal variations of particle fluxes in the deep subtropical and tropical North Atlantic: Eulerian versus lagrangian effects. *J Geophys Res* 93:6857–6862.
25. Kortzinger A (2003) A significant CO2 sink in the tropical Atlantic Ocean associated with the Amazon River plume. *Geophys Res Lett* 30, doi:10.1029/2003GL018841.
26. Cooley SR, Coles VJ, Subramaniam A, Yager PL (2007) Seasonal variations in the Amazon plume-related atmospheric carbon sink. *Global Biogeochem Cycles* 21, doi:10.1029/2006GB002831.
27. Kemp AES, Pearce RB, Koizumi I, Pike J, Rance SJ (1999) The role of mat-forming diatoms in the formation of Mediterranean sapropels. *Nature* 398:57–61.
28. An CN (1971) Atlantic Ocean Phytoplankton south of the Gulf of Guinea on profiles along 11 and 14S. *Oceanology* 6:896–901.
29. Voss M, Bombar D, Loick N, Dippner J (2006) Riverine influence on nitrogen fixation in the upwelling region off Vietnam, South China Sea. *Geophys Res Lett* 33, doi:10.1029/2005GL025569.
30. Carpenter EJ, Subramaniam A, Capone DG (2004) Biomass and primary productivity of the cyanobacterium, *Trichodesmium* spp, in the tropical N Atlantic Ocean. *Deep-Sea Res I* 51:173–203.
31. Capone D, *et al.* (2005) Nitrogen fixation by *Trichodesmium* spp: An important source of new nitrogen to the tropical and subtropical North Atlantic Ocean. *Global Biogeochem Cycles* 19, doi:10.1029/2004GB002331.
32. Wright SW, *et al.* (1991) Improved HPLC method for the analysis of chlorophylls and carotenoids from marine phytoplankton. *Mar Ecol Progress Ser* 77:183–196.
33. Dickson AG, Goyet C, eds (1997) *Handbook of methods for the analysis of the various parameters of the carbon dioxide system in seawater*. (DOE, Washington, DC) ORNL/CDIAC-74 Version 2.1.
34. Bruland KW, Coale KH, Mart L (1985) Analysis of seawater for dissolved cadmium, copper, and lead: An intercomparison of voltametric and atomic adsorption methods. *Mar Chem* 17:285–300.
35. Karl DM, Tien G (1992) A sensitive and precise method for measuring dissolved phosphorus in aquatic environments. *Limnol Oceanogr* 37:105–116.

Supporting Information

Subramaniam *et al.* 10.1073/pnas.0710279105

SI Text

Carbon and Nitrogen Fixation. Carbon fixation by *Trichodesmium* was determined by the ^{14}C-uptake method (1) and nitrogen fixation by the C_2H_2 reduction method (2). Carbon fixation by the DDA was measured along with all other phytoplankton and is reported as bulk primary production. Biogenic silica production rates were then used to estimate the productivity of diatoms. *Richelia* N_2-fixation rates were measured before concentrating samples by either direct collection onto 40-μm Nitex with gentle backwashing into a clean beaker and/or reverse filtration. When colonial *Trichodesmium* was present in the water along with the diatoms, the water was prescreened through a 202-μm mesh to remove it. The concentrate was diluted to a specific volume and checked under a microscope for the presence of other organisms. Samples were assayed by C_2H_2 reduction at the range of irradiances in on-deck incubators (2). We also measured total nitrogen fixation using $^{15}N_2$ uptake on unscreened volumes of unconcentrated water at select stations. The rates obtained by this technique are highlighted in Table S2 and showed nitrogen-fixation rates at stations dominated by *Richelia* to be as high as 12 mmol of N m^{-2} d^{-1}, 10–100 times higher than that obtained by C_2H_2 reduction in this study but comparable with the rates obtained by C_2H_2 reduction without any preconcentration on a previous cruise in 1996 (3). The lower C_2H_2 reduction could be due to the handling required to isolate *Richelia*.

Chlorophyll a. Samples were filtered on to GF/F, 25-mm glass fiber filters and stored in liquid nitrogen. Pigments were separated by a HPLC with a ODS-2 C18 column using a three-solvent gradient system at a flow rate of 1 ml/min. (4).

DIC. A simple conservative mixing model using alkalinity and salinity was developed to calculate the proportions of Amazon plume water and seawater in a given sample, remove the effects of the river contribution, and calculate the oceanic component (5). The difference between the expected oceanic and observed DIC concentrations was attributed to biological drawdown (6).

Salinity Classification. Although we have used a simple salinity-based classification scheme, the WTNA is an extremely complex and dynamic system with high spatial heterogeneity consisting of eddies, freshwater filaments, and a constantly changing river plume. Instead of a simple seasonal control, surface properties related to the dynamics of the river plume significantly influenced phytoplankton response. Even within the river plume, surface salinity alone was not a perfect predictor of community structure. Because river-borne nutrient concentrations vary with seasonal discharge (7), coastal diatoms and higher NO_3 concentrations could be found at higher salinity ($\approx$30–31) stations in the spring, presumably because of higher initial nutrient concentrations at the river mouth, whereas in the summer, many stations with salinities as low as 28 had no detectable NO_3 and were devoid of coastal diatoms but had relatively high counts of *Trichodesmium*.

Area of the Plume. We used the relationship between salinity and K490, the attenuation coefficient, (8) to calculate the area of WTNA covered by the Amazon River Plume. The area for each month and the corresponding images are provided in Table S1.

Statistics. Matlab Statistical Toolbox was used to perform the Wilcoxon rank sum and Kruskal–Wallis tests. The data for each station of the aggregated parameters in Table 1 are given in Table S2. Systat software was used for the principal-component analysis.

1. Carpenter EJ, Subramaniam A, Capone DG (2004) Biomass and primary productivity of the cyanobacterium, Trichodesmium spp., in the tropical N. Atlantic Ocean. *Deep Sea Res I* 51:173–203.
2. Capone D, *et al.* (2005) Nitrogen fixation by *Trichodesmium* spp.: An important source of new nitrogen to the tropical and subtropical North Atlantic Ocean. *Global Biogeochem Cycles* 19:doi:10.1029/2004GB002331.
3. Carpenter EJ, *et al.* (1999) Extensive bloom of a N2-fixing diatom/cyanobacterial association in the tropical Atlantic Ocean. *Mar Ecol Progress Ser* 185:273–283.
4. Wright SW, *et al.* (1991) Improved HPLC method for the analysis of chlorophylls and carotenoids from marine phytoplankton. *Mar Ecol Progress Ser* 77:183–196.
5. Cooley SR, Yager PL (2006) Physical and biological contributions to the western tropical North Atlantic Ocean carbon sink formed by the Amazon River plume. *J Geophys Res C* 111, doi:10.1029/2005JC002954.
6. Cooley SR, Coles VJ, Subramaniam A, Yager PL (2007) Seasonal variations in the Amazon plume-related atmospheric carbon sink. *Global Biogeochem Cycles* 21, doi:10.1029/2006GB002831.
7. DeMaster DJ, Aller RC (2001) Biogeochemical Processes on the Amazon Shelf: Changes in Dissolved and Particulate Fluxes During River/Ocean Mixing. in *Biogeochemistry of Major World Rivers*, eds Degens ET, Kempe S, Richey JE (Wiley, New York), pp 323–347.
8. Del Vecchio R, Subramaniam A (2004) Influence of the Amazon River on the surface optical properties of the western tropical North Atlantic Ocean. *J Geophys Res* 109, doi:10.1029/2004JC002503.

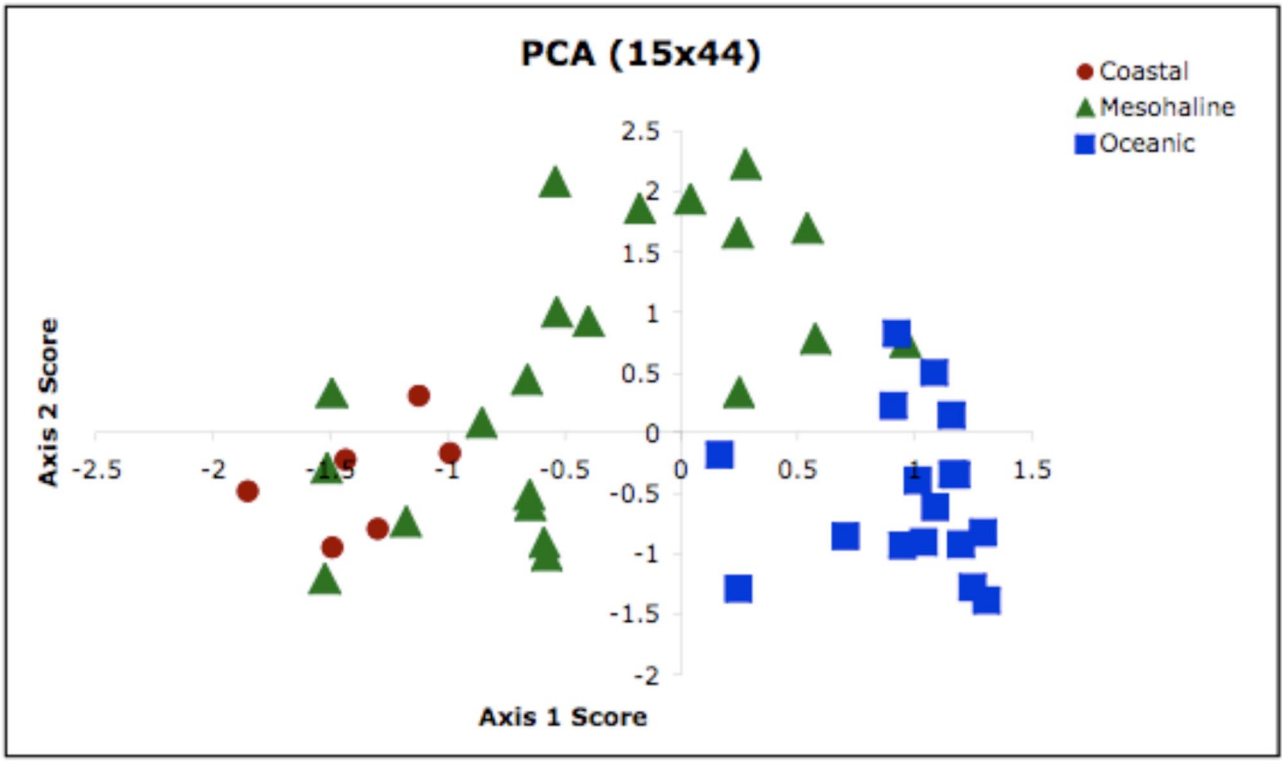

Fig. S1. Component loading scores for the first (*x*) and second (*y*) axes of the PCA for each station. The *x* axis describes the coastal–oceanic gradient, with the coastal stations having a negative score, whereas the oceanic stations have a positive score.The *y* axis describes the DDA blooms, stations with high *Richelia*, N_2-fixation rates, and low DIC have positive scores.

Table S1. Area of the Amazon River plume as detected by SeaWiFS K490 monthly climatology

Month	km^2	m^2	mol/month
January	294,435	2.9E+11	5.9E+10
February	297,675	3.0E+11	6.0E+10
March	361,341	3.6E+11	7.3E+10
April	705,267	7.1E+11	1.4E+11
May	1,053,000	1.1E+12	2.1E+11
June	1,283,445	1.3E+12	2.6E+11
July	1,307,907	1.3E+12	2.6E+11
August	1,232,820	1.2E+12	2.5E+11
September	885,897	8.9E+11	1.8E+11
October	490,941	4.9E+11	9.9E+10
November	277,101	2.8E+11	5.6E+10
December	252,963	2.5E+11	5.1E+10

Total annual new carbon (mol/yr): 1.7 ± 0.6 E + 12.

Table S3. A principal-component analysis (performed on log+1 transformed data) was applied on data from the 44 stations where every one of 15 key variables (listed below) were measured

	Axis 1	Axis 2	Axis 3	Axis 4
%VAR EXP:	35	19	13	7
MLD	**0.901**	-0.218	-0.238	-0.034
TEMP	**-0.866**	0.066	0.243	0.147
SAL	**0.844**	-0.016	0.081	-0.150
LIGHT	**0.798**	-0.386	0.322	0.072
DSI	**-0.767**	-0.327	0.069	0.226
WIND	**0.715**	0.293	-0.219	-0.099
CHLA	**0.655**	0.393	0.093	0.196
RICHEL	-0.003	**0.913**	-0.020	0.105
N2FIX	0.239	**0.748**	0.399	-0.047
DICR	0.454	**-0.633**	0.170	0.288
SRP	0.375	0.204	**-0.772**	0.055
TRICHO	0.156	0.318	**0.734**	-0.387
BSI	-0.430	0.467	**-0.516**	0.061
PRIMPROD	0.474	0.166	0.137	**0.727**
DFE	-0.127	0.277	0.281	**0.428**

The PCA generated four axes that explained 74% of the system variance. Axis 1 (35%) described the river–ocean gradient correlated with mixed layer depth (MLD), sea surface temperature (TEMP), sea surface salinity (SAL), 1% light depth (LIGHT), dissolved silicon (DSI), wind speed (WIND), and chlorophyll *a* (CHLA). Axis 2 (19%) described the mesohaline DDA blooms and correlated with integrated *Richelia* abundance (RICHEL), river-corrected DIC (DICR), integrated N_2 fixation (N2FIX). Axis 3 (13%) correlated with integrated *Trichodesmium* abundance (TRICHO), surface soluble reactive phosphorus (SRP), and integrated biogenic silica (BSI). The fourth axis (7%) correlated with total integrated primary production (PRIMPROD) and dissolved iron (DFE), suggesting that iron was not limiting production in this region. The correlations shown are the component loadings from SYSTAT, i.e., the correlation of each variable to the component axis. The key result is that the largest nonconservative changes in DIC and nitrogen-fixation rates are associated with high *Richelia* biomass on Axis 2. PCA was conducted by using SYSTAT.

Other Supporting Information Files

Table S2 (XLS)